



Hydrogeological conceptual model of andesitic watersheds revealed by high-resolution geophysics

Benoit Vittecoq^{1,2}, Pierre-Alexandre Reninger³, Frédéric Lacquement³, Guillaume Martelet³, Sophie Violette^{2,4}

5 ¹BRGM, 97200 Fort de France, Martinique

²ENS-PSL Research University & CNRS, UMR.8538 – Laboratoire de Géologie, 24 rue Lhomond, 75231 Paris France

³BRGM, F-45060 Orléans, France

⁴Sorbonne Université, UFR.918, F75005, Paris France

Correspondence to: Benoit Vittecoq (b.vittecoq@brgm.fr)

10 **Abstract.** We conducted a multidisciplinary study at the watershed scale of an andesitic-type volcanic island in order to better characterize the hydrogeological functioning of aquifers and to better evaluate groundwater resource. A helicopter-borne TDEM survey was conducted in 2013 over Martinique Island in order to investigate underground volcanic structures and lithology, characterized by high lateral and vertical variability, and resulting in a very high heterogeneity of their hydrogeological characteristics. Correlations were made on three adjacent watersheds between resistivity data along flight
15 lines and geological and hydrogeological data from 51 boreholes and 24 springs, showing that the younger the formations, the higher their resistivity. Correlation between resistivity, geology and transmissivity data of three aquifers is attested: the older the formation, the lower its resistivity, and the higher its transmissivity. Moreover, we demonstrate that the main geological structures lead to preferential flow circulations and that hydrogeological watershed can differ from topographical watershed. The consequence is that even if the topographical watershed is small, underground flow circulations can add significant amount
20 of water to river watershed's water balance. This effect is amplified when lava domes and their roots are situated upstream, as they present very high hydraulic conductivity leading to deep preferential groundwater flow circulations. We also reveal, unlike basaltic-type volcanic islands, that hydraulic conductivity increases with age in this andesitic-type volcanic island. This trend is interpreted as the consequence of tectonic fracturing associated to earthquakes in subduction zones associated to andesitic volcanic islands. Finally, our approach allows characterizing in detail the hydrogeological functioning and identifying
25 the properties of the main aquifer and aquitard units, leading to the proposition of a hydrogeological conceptual model at the watershed scale. This working scale seems particularly suitable due to the complexity of edifices, with heterogeneous geological formations presenting high lateral and vertical variability. Moreover, our study offers new guidelines for accurate correlations between resistivity, geology and hydraulic conductivity for volcanic islands. Finally, our results will also help stakeholders toward a better management of water resource.



1 Introduction

Water resources management on volcanic islands is challenging as these territories are often densely populated, subject to several natural hazards (volcanism, earthquakes, tsunamis, landslides, erosion and sea level rise...), and with increasing water demands (for irrigation, drinking water...) or excessive intake in rivers or aquifers. Understanding the hydrogeological functioning of these islands is thus a major issue to achieve a sustainable management of their water resources. Hydrogeology of volcanic islands is challenging taking into consideration the complexity of these edifices and the difficulties encountered when acquiring accurate in-situ data (such as steep slopes, tropical vegetation, few access tracks, distance from laboratories, extreme climatic and hydrometric conditions for equipment...).

Historically, basaltic islands were the most studied: (e.g. Hawaii: Peterson, 1972; Macdonald et al., 1983; Canarian Islands: Custodio, 1975; Custodio et al., 1988; Custodio, 2005; Iceland: Sigurðsson and Einarsson, 1988; Réunion Island: Violette, 1997; Join et al., 2005; Azores Islands: Cruz and Silva, 2001; Cruz, 2003; Galapagos Islands: Violette et al., 2014; Jeju Island: Hamm et al., 2005; Won et al., 2005, 2006; Hagedorn et al., 2011; or Mayotte: Vittecoq et al., 2014), leading to several hydrogeological conceptual models, essentially at the island scale, each model being intrinsically linked to the dynamics of volcanism activity, to the number and history of volcanoes and their effusive and rest phases, generating a more or less complex geometry within which water infiltrates and circulates in a complex pattern.

Andesitic islands in subduction zones, and especially the Caribbean ones, are less known and a limited number of hydrogeological studies work have been conducted and published in these archipelagos, mainly at the island scale (e.g. Unesco, 1986, Falkland and Custodio, 1991, Davies and Peart, 2003; Gourcy et al., 2009, Vittecoq et al., 2010, Robins, 2013; Hemmings et al., 2015). Charlier et al. (2011) show the interest in working at the watershed scale to define a hydrogeological scheme of a tiny site (45 ha) in Guadeloupe Island. Hydrogeological analyses at several scales are indeed essential, especially for this type of volcanism, characterized by heterogeneous geological formations, with alternation between intense eruptive phases marked by andesitic lava flows, pyroclastic flows, lahars, etc. interspersed with quieter phases marked by the dismantling of the volcano with debris avalanches and meteoric and alluvial erosion (Westercamp et al., 1989, 1990). Furthermore, andesitic stratovolcanoes show volcanic facies trends with variation and lateral distribution between central, proximal, medial and distal zones, depending on the valley and interfluvial dynamics (Vessel and Davis, 1981; Bogie and Mackenzie, 1998; Selles et al., 2015). Moreover, meteorological and hydrothermal weathering processes are superimposed on these lithological heterogeneities. This high lateral and vertical geological variability thus induces a very high heterogeneity of their hydrogeological characteristics. As shown by most of these studies, without in-depth data, it is not possible to understand relevant geological structures and consequently to understand the hydrogeological functioning.

Recently, heliborne geophysical surveys (e.g. Sorensen and Auken, 2004) started providing new regional in-depth data, which contribute to solving this scientific and technical challenge. High-resolution heliborne EM (ElectroMagnetic) resistivity data provide information down to the first hundred meters along flight lines, and allow a continuous imagery of resistivity variations. Geological structures and hydrogeological properties can then be interpreted from these geophysical data to



determine and constrain accurate conceptual models. To be relevant, and because resistivity is clearly not a univocal parameter, this dataset analysis must be constrained with as much direct observation data (outcrop, borehole geological log, hydraulic conductivity data...) as possible (see for instance Vittecoq et al., (2014) for Mayotte basaltic island).

Vittecoq et al., 2015, in studying an andesitic coastal aquifer in Martinique, demonstrate the relevance of working and analysing airborne EM data at the aquifer scale, to characterize geological and hydrogeological heterogeneities inside a 15 Ma old geological formation. At this scale, this approach is corroborated thanks to a very long term pumping experiment. The working scale should indeed be sufficiently fine to be relevant to the structural specificities of these andesitic volcanic islands. However, working scale should also include surface and hydrogeological watersheds to integrate water balance estimation, interaction between groundwater and surface water, potential contribution of different aquifers and vertical downward transfers, for a comprehensive view of the water cycle, so that stakeholder can use the results for a sustainable management of water and energy resources.

Considering these issues, we conducted a multi-disciplinary approach at a watershed scale, based on the correlation of geological, hydrological, hydrogeological and airborne Time Domain ElectroMagnetic (TDEM) data. We focus on a few strategic watersheds situated in Martinique, a predominantly andesitic volcanic island (Westercamp et al., 1989) located in the Lesser Antilles volcanic arc, in the subduction zone between the Atlantic plate and the Caribbean plate. The goal of our study is thus to: (i) characterize the structure and hydrogeological functioning of Martinique andesitic aquifers at the watershed scale, (ii) show the influence of geological structures on groundwater flows and the consequence on the interactions between rivers and aquifers, (iii) assess the adequacy and difference between hydrological watershed and hydrogeological watershed, (iv) propose a conceptual model at the watershed scale, and (v) strengthen the hypothesis of Vittecoq et al., 2015 that, in contrast with the basaltic islands, age is not the key factor controlling hydraulic conductivity.

2 Martinique Island and studied watersheds

2.1 Site location and climate

Martinique Island (Fig. 1) is the largest volcanic island (1,080 km²) of the Lesser Antilles Archipelago. Its relief is mountainous in the North (highest volcano at 1,397 m) and gentler in the South (highest hill at 504 m). Rainfall is characteristic of a humid tropical climate controlled by the trade winds and orographic effects (Guiscafre, 1976; Vittecoq et al., 2010), with the rainy season between July and November and the dry season between January and April, interspersed with fluctuating transition periods. Annual temperatures vary between 18°C and 32°C at Fort-de-France and an East trade wind regime ensures relatively constant ventilation. Average annual precipitation is high in the northern part, reaching 5,000 to 7,000 mm per year at the summits, and between 1,200 and 1,500 mm per year in the south.

The three studied watersheds (Fig. 1) are located just near the capital city of Fort-de-France whose agglomeration includes half the population of the island (388,000 inhabitants on the island in 2014). Tree dams are located on the Case Navire River, and provide an average of $5.9 \cdot 10^6$ m³ per year to the agglomeration. During dry seasons, the river is often dry over several



hundred meters downstream of the dams, causing strong environmental impacts. Consequently, scientific researches are expected to understand the hydrological and hydrogeological functioning of this area, in order to propose alternative water resources management.

2.2 Geology

- 5 The volcanic activity of Martinique Island (Westercamp et al., 1989; Germa et al., 2010, 2011), which began more than 25 Ma ago, is characterized by a succession of many volcanic formations, mainly andesitic, set up from a dozen principal volcanic edifices, active during successive phases, with alternating periods of construction and erosion, sometimes contemporary. The geology of the study area (Fig. 2A) is concerned with two distinct phases and volcanic edifices (Westercamp et al., 1989): the Morne Jacob shield volcano and the Carbets volcanic complex (Fig. 2B). The Morne Jacob Shield Volcano is the largest
- 10 edifice on the island and lasted 3.3 Ma. Given its position, offset from the pre-existing reliefs, the first phase is first submarine then aerial. First phase formations are mostly weathered, because of a long period of rest and erosion of at least 1 Ma before the next phase. The strong aerial effusive volcanic activity of the second phase of the Morne Jacob volcano is witnessed on the field by massive flows (2α) up to 200 m thick. The Carbets volcanic complex develops on the western flank of the Morne Jacob shield volcano and lasted 1.3 Ma with four main aerial phases.
- 15 Despite this detailed knowledge of the nature and location of the geological formations constituting the watersheds, and their lateral extension at the 1:50000 scale; it remains difficult to have a precise and 3D vision of their geometries and relationship at depth.

2.3 Hydrogeology

- The position of the springs and the available drilling data (Fig. 1 and 2) suggest that aquifers could be associated with almost
- 20 every volcanic phase of each edifice.

2.3.1 Cold springs and streams

- Springs (Fig. 1 and 2) are located mainly in the upper part of the watersheds (between 204 and 663 m amsl). Springs water discharge are relatively small, most of the time a few liters per second. They are associated to three main geological formations (Fig. 3A and 3B). Nine springs, situated between 440 and 580 m amsl, emerge from andesitic and dacitic dome and lava flows
- 25 $^9\alpha$ bi (0.9 Ma). This geological formation is the last main event of the Pitons du Carbet Complex and strongly marks the landscape with several monolithic domes. In addition to observed springs, many perennial rivers flow from these peaks, so the aquifer that feeds these springs and rivers can be considered as an important perched aquifer. Six springs, emerging between 204 and 660 m amsl, are associated to andesitic lavas $^2\alpha$ (2.2-2.8 Ma), and four springs, emerging between 296 and 350 m amsl, are associated to basaltic lavas $^1\beta$ ol (4-5.5 Ma). These springs are mostly situated at slope foot, at slope breaks or at the
- 30 top of gullies. Andesitic lavas $^2\alpha$ and basaltic lavas $^1\beta$ ol are thus permeable and considered as aquifer formations. Finally, three



other springs emerge from secondary aquifers, two from andesitic lavas ⁶α and one from debris flow (⁶B) both associated to the first phase of construction of the old Carbet (2 Ma).

2.3.2 Thermal springs

Two thermal springs, Didier (32°C – 1850 μS/cm) and Absalon (36°C – 1730 μS/cm) are situated in the middle of the Case Navire watershed (Fig. 1 and 2). Their waters are mainly bicarbonated Ca-Na-Mg and are associated with emissions of magmatic CO₂ (Gadalia et al., 2014). The geochemical model (Gadalia et al., 2014) proposes an evolution in three stages: (1) deep mixing between water of meteoric origin and marine water (around 0.1%), during a first partial chemical and isotope equilibrium; (2) water-rock and magmatic CO₂ interaction at medium temperature (90-140°C) in a residual geothermal system, and (3) mixing with meteoric waters during the ascent, at a lower temperature.

10 2.3.2 Boreholes

Fifty-one boreholes (Table S1) were drilled on these watersheds or in the close vicinity (Fig. 1D and 2A). Transmissivity data are available for 19 boreholes (¹βol, ¹α, ²α, and ⁶B) and vary by two orders of magnitude between 1.10⁻⁵ m² s⁻¹ and 1.10⁻³ m² s⁻¹, with an average value of 5.0 10⁻⁴ m² s⁻¹ (standard deviation: 3.0 10⁻⁴ m² s⁻¹). Hydraulic conductivity vary between 2.3 10⁻⁷ m s⁻¹ and 3.3 10⁻⁵ m s⁻¹ with an average value of 1.4 10⁻⁵ m s⁻¹ (standard deviation: 8.5 10⁻⁶ m s⁻¹). As aquifers are fissured or fractured with heterogeneities along the screen height, and as data were calculated by dividing transmissivity by the height of the screened saturated aquifer, calculated hydraulic conductivities have to be considered as minimum values.

Piezometric level measurements (Fig. 3A) shows that the piezometric level is on average seven meters below ground level and attests that the hydrogeological functioning is not marked by a basal groundwater body with low hydraulic gradient. In addition, two main typology of aquifer are distinguished on Fig.3B: on one hand perched aquifers with springs located in altitude above 400 m amsl and on the other hand aquifers crossed by boreholes in the valleys with water level close to the ground level.

Piezometric levels monitoring (Fig.4) put in evidence unconfined aquifers (Piezometers 1, 2 and 4), with annual dynamics and well-defined seasonal cycle (with fluctuations between 1 and 2 m): low groundwater levels occur during dry seasons (April to July) and high ones during rainy seasons (August to December). In contrast, piezometer 3 (situated 1 kilometer above piezometer 2), characterizes a confine aquifer with multiannual dynamics, with a minor influence of seasonal cycle.

25 2.3.1 Water balance

The Alma watershed is the highest and smallest one, located upland, and is exclusively tropical forest. This watershed is equipped with a gauging station with valid data since July 2010 (specific discharge of about 112 l s⁻¹ km⁻²). Water balance calculation (Fig. 5) put in evidence that the difference between total effective rainfall and average annual flow in the Alma River is about 2.3 10⁶ m³/year (18% of effective rainfall volume). This volume of water (1) infiltrates in depth and / or (2) joins another stream / nearby hydrological watershed in case of the hydrogeological catchment area has differences with the topographic catchment. This volume infiltrated in depth or flowing towards an adjacent catchment area is therefore to be



considered as a minimum value, as measured rainfall gauges are situated at elevations not exceeding 600 m whereas the watershed peak culminates at 1,197 m. The national climatic agency (Météo-France) considers that values of 6,000 to 7,000 mm of rain per year are quite possible values on the summits. Considering this highest value, and the different uncertainties on the water budget parameters, the deep infiltrated volume could reach a maximum of $8 \cdot 10^6 \text{ m}^3/\text{year}$.

5 The Fond Lahaye watershed culminates at 532 m of elevation and its stream joins the sea 4 km downstream. Since there is no gauging station on this river, it is difficult to define a water balance. In the maximalist hypothesis where 100% of the effective rainfall returns to the river, its maximum specific discharge would be of about $11 \text{ l s}^{-1} \text{ km}^{-2}$ (corresponding to 10% of the nearby Alma watershed specific discharge).

The Case-Navire watershed culminates at 1,197 m of elevation (Piton Lacroix) and its stream joins the sea 10 km downstream.
10 A gauging station is situated on the Case Navire River few hundred meters before reaching the sea (Fig.1 and 2A). Its upstream part is divided into two sub-basins (Duclos and Dumauzé rivers) that meet 5 km before reaching the sea (Fig. 3B). Three dams are located in the upstream part of the Case Navire River (one on the Dumauzé River and two on the Duclos River, cf. Fig 1). The only available data is a cumulative annual volume of the three dams on arrival at the main distribution tank: the annual volume is $5.9 \cdot 10^6 \text{ m}^3$ per year, corresponding to an average of $16,300 \text{ m}^3$ per day (and corresponding to 19% of the annual effective rainfall).
15 During dry seasons, the river is often dry downstream of the dams, causing strong environmental impacts. The gauging station, situated 5 to 6.5 km downstream the dams has valid data since 2012, allow calculating water balances (Fig. 5). The supposed natural flowrate of the Case Navire River is then about $18.7 \cdot 10^6 \text{ m}^3$ per year, corresponding to 60% of the annual effective rainfall, by adding water abstraction volume by dams. Consequently, the volume of groundwater circulating in this watershed that does not return to the river is about $12.4 \cdot 10^6 \text{ m}^3/\text{year}$. This volume may infiltrate in depth and
20 circulates in the aquifers, to another watershed or flows into the sea.

These water balances calculations put in evidence the main key component of hydrological cycle of each watershed and provide first evaluations of groundwater budget. In particular, they reveal significant quantities of deep infiltrated water (14.7 to $20.4 \cdot 10^6 \text{ m}^3/\text{year}$), equal to two or three times the actual surface water intake in the Case Navire River. As no deeper or detailed analyses of these hydrogeological data were performed until now, there is a necessity to better understand aquifer nature and
25 hydrodynamic characteristics, extension, thickness and groundwater preferential flows and interactions with rivers, and to locate recharge areas, in order to propose appropriate hydrogeological conceptual models, necessary to a sustainable management of water resources.

3 – Heliborne TDEM method

Our methodology is based on a multidisciplinary approach combining geology, hydrogeology and a heliborne TDEM
30 geophysical survey, in order to put in evidence relationships between ground-based punctual geological and hydrogeological data, and in depth geophysical information derived all over the area.



3.1 The survey

A heliborne TDEM survey was conducted from February to March 2013 with the SkyTEM 304 system (Sørensen and Auken, 2004) over the entire Martinique Island. This survey, fully described by Deparis et al., 2014 and Vittecoq et al., 2015, was supervised by BRGM (the French geological survey) for geological and hydrogeological purposes. Over the studied
5 watersheds, the survey was flown mainly along the N-S direction with 400 m line spacing, and along the W-E direction with 4,000 m line spacing. The spacing between each EM sounding along flight lines is approximately 30 m. In the lower part of the watershed less to no data have been acquired because of the urbanization. Finally, 13,596 TDEM soundings were processed in the study area. The TDEM method allows imaging the conductivity/resistivity contrasts of the subsurface, inducing eddy currents in the ground (Ward and Hohmann, 1988). Locally, the depth of investigation of the method depends on the emitted
10 magnetic moment, the bandwidth used, the subsurface conductivity and the signal/noise ratio (Spies, 1989). In this study, the average depth of investigation is around 150-200 m.

3.2. TDEM data processing

The ground clearance of the loop was obtained degrading an available 1 m Digital Elevation Model to a 25 m grid (consistently with the AEM footprint) and subtracting it to the DGPS altitude; we did not use the data from the laser, which proved to be
15 noisy in such rough relief environment. Tilt measurements were processed taking into account the local topography in order to consider an effective tilt at each TDEM data location (Reninger et al., 2015). As part of an environmental study in an anthropogenic area, particular attention was paid to properly remove noise from the TDEM data. They were processed with a singular value decomposition filter (Reninger et al., 2011). In addition, a trapezoidal stack (Auken et al., 2009) was applied on the data. The stack size is being adapted to the noise level along flightlines (Reninger et al., 2018). Finally a manual editing
20 was performed, mainly to remove remaining inductive/galvanic coupling noises. In order to improve the coverage of the dataset, good quality portions of ferry lines were also considered during the processing (Reninger et al., 2018). Data were then inverted using the Spatially Constrained Inversion algorithm (SCI) (Viezzoli et al., 2008). Each TDEM data was interpreted as a 1-D earth model (EM sounding) divided into n layers, each one being defined by a thickness and a resistivity. During the inversion, constraints were applied vertically and horizontally on nearby soundings (independently of the flightlines and the
25 ground clearance). Results were obtained with a smooth inversion (consisting of 23 layers from 0 to 200 m depth). This inversion method is effective to image complex geological structures with the lowest dependency on the starting model. In addition, altitude of the transmitter was inverted for, and the Depth Of Investigation (DOI) was evaluated, as a final step of the inversion (Christiansen and Auken, 2012). Figures 1 and 2 display the position of the TDEM data considered as usable after the processing step and which were subsequently inverted.



4 – Resistivity profiles and correlations between resistivity, geological and hydrogeological data

Five resistivity profiles obtained inverting TDEM data are provided on figures 6 and 7 (localization in Fig. 2), intersecting the study area. Confronting these profiles with geological and hydrogeological data (springs, boreholes, observations and outcrops, geological map...), the TDEM data can be interpreted in terms of geological or hydrogeological contrasts, and evidence the main internal geological structures and associated aquifers, at depth up to around 200 m. Thus, as exposed by Vittecoq et al., (2014) and Vittecoq et al., (2015), geological and transmissivity data of each borehole can be compared to the closest TDEM sounding in order to get information on the resistivity of the aquifers and aquitards and better constrain their extension and thickness. However, in such particularly rugged and contrasted environment, it must be paid attention how this comparison is achieved, mainly in terms of distance and elevation. This was done on 18 boreholes. They are located at an average distance of 35 m (with a maximum distance of 90 m) to the closest EM sounding, with a difference in elevation less than 10 m. At each of these TDEM soundings, we looked at the average of the resistivity falling in each associated borehole geological formations. To complete aquifer characterization, a specific analysis was conducted on the springs. Resistivity values located upstream springs in the interpreted aquifer formation were manually extracted from the resistivity models.

Figure 8A displays borehole (BR) and spring (SR) aquifer resistivity ranges. Alluvial deposits display a relatively large resistivity range (12-74 ohm m) because of the heterogeneity of alluvial materials (in terms of granulometry, nature, ages...). Except for alluvial deposits, a good correlation appears between resistivity and the age of the geological formations, showing the relationship between weathering process and resistivity: the older the formation, the lower its resistivity. Correlation between resistivity, geology and transmissivity data (Fig. 8B) also displays a trend: the older the formation, the lower its resistivity, and the higher its transmissivity. In particular, the relatively large resistivity and hydraulic conductivity range for andesitic lavas 2 α should be related to their intrinsic heterogeneity.

These correlations demonstrate the necessity and advantage of coupling hydrogeological data (springs, boreholes...), geological and geophysical data for an advanced interpretation of resistivity data, as such information is scarce in volcanic islands environments and because alone resistivity data does not allow differentiating age, nature of geological formations or aquifer identification.

5 – Hydrogeological conceptual model

Our methodology and associated correlations allows identifying and characterizing the main aquifer and aquitard formations (synthetized in table 1) as well as their lateral extent and thickness, enabling the construction of a hydrogeological conceptual model at the hydrogeological watershed scale. This conceptual model, synthetized on Fig. 9, characterize the structure and hydrogeological functioning of andesitic aquifers at the watershed scale, and highlight the influence of geological structures on groundwater flows and the consequence on the interactions between rivers and aquifers. Joint analysis of water balance and geological structure also allows putting in evidence the differences between hydrological watershed and hydrogeological watershed.



5.1 The upper major perched aquifer of andesitic domes

The conceptual model is marked by the presence of andesitic domes and lava flows ($^{\circ}\alpha_{bi}$), occupying the upper part corresponding to half of Case Navire watershed and the entire Alma watershed. Water balance calculated on Alma River suggests that 85% of effective rainfall (Reff) infiltrates in these andesitic domes. Considering the high resistivity values of the domes (Cf. Fig. 8A, springs resistivity analysis: 150-500 ohm m) and in comparison with other volcanic islands (d'Ozouville et al., 2008; Pryet et al., 2012; Vittecoq et al., 2014), it is assumed that these andesitic domes ($^{\circ}\alpha_{bi}^D$) are highly fissured and fractured, conferring a great hydraulic conductivity to this aquifer. Given the rooting of endogenous domes within the volcano, and as shown thanks to the water balance calculation (Fig. 5), up to 40% of Reff seeps in depth within domes roots, through fissures and fractures, and recharge underlying aquifers.

In addition, the unsaturated zone should present significant thickness, and since some springs observed have relatively low flow rates, we consider that they could emerge thanks to small and low hydraulic conductivity horizons, such as paleo-soils, or geological heterogeneities (for instance between $^{\circ}\alpha_{bi}$ and underlying formation), or structural discontinuities. The main rivers have their sources in this important perched aquifer, with significant flow rate (as show in Fig. 5, for instance the Alma River specific discharge is $112 \text{ l s}^{-1} \text{ km}^{-2}$). On the western and eastern topographic ridges of the Case Navire River watershed, andesitic lava flows ($^{\circ}\alpha_{bi}^C$) also constitute the first aquifer receiving rainfall and from which flows some non-perennial springs during the rainy season, and few perennial springs during the dry season.

5.2 The lower aquifer of andesitic lavas

In this conceptual model the upper major perched aquifer, described above, underlies the second main aquifer of thick andesitic lavas $^2\alpha$, marked by a relatively “smooth” morphology or paleo-topography of their top, consistent with the structure of lava cooling along a shield volcano. Hydraulic conductivity data dispersion over two orders of magnitude is in agreement with the heterogeneity of these andesitic lavas. The various facies that were observed at the outcrop are: (1) auto-brecciated breccias and lavas, (2) massive facies more or less fractured according to the cooling rate of the lava, (3) facies with flow structures showing significant horizontal cracking parallel to the substratum, and (4) breccias and scorias associated with the base of the lava flow. Tectonic fracturing superimposes on these heterogeneities and can contribute to maintain and develop the hydraulic conductivity of volcanic formations, as shown by Vittecoq et al., (2015). In this type of andesitic formation, boreholes can also be dry, if no fissured or permeable zone is intersected.

The recharge of this aquifer is quite atypical as in the upper part of Case Navire and Dumauzé watersheds, effective rainfall is high, and permeable andesitic domes and lava flows $^{\circ}\alpha_{bi}$ overly andesitic lavas $^2\alpha$. As suggested by numerous springs in the border of $^{\circ}\alpha_{bi}$, and the low flowrates observed in the two Fond Baron boreholes screened into andesitic lavas $^2\alpha$ (Senergues, 2014), effective rainfall infiltration into $^2\alpha$ should be limited as paleo-soils and the hydraulic conductivity contrast between the two formations could act as semi-permeable hydraulic obstacles. In the lower part of the watersheds, effective rainfall is limited



(200 to 800 mm/year) compared to the upper part, and furthermore the plateau located on both sides of the rivers are overlain by low hydraulic conductivity breccias. Effective rainfall infiltration towards andesitic lavas $^2\alpha$ is thus also small in the lower part of the watersheds. Then, the recharge of this aquifer should follow four main steps. Firstly, effective rainfall deeply infiltrates in the aplomb and in the rooting of andesitic domes $^9\alpha$ bi. Secondly, as andesitic lavas $^2\alpha$ were crossed through faulting by $^9\alpha$ bi lavas, this deeply infiltrated water then flows deeper towards andesitic lavas $^2\alpha$, thanks to geological heterogeneity inside the old volcanic chimney. Thirdly, groundwater flows into andesitic lavas $^2\alpha$ and lastly, the $^2\alpha$ aquifer, incised by the river, allows this deeply infiltrated water to be drained by the river and the sea.

5.3 The regional aquitard

Hyaloclastites 1H , mainly observable on Fig. 6 (C3) and Fig. 7 (C4 and C5) at altitudes below 100 m amsl, are the lower boundary of the watersheds and more generally, of a major northern part of the island. On Fig. 6 (C2), they are suspected between 200 and 300 m amsl on the east of the cross-section, probably due to the displacement generated by major faults: this topographical limit is interpreted by Boudon et al., 2007 as the eastern limit of a large flank collapse with a horseshoe-shape structure opened westward. The state of weathering observed on the outcrop in the Case Navire River, associated to their very low resistivity, lead to consider the hyaloclastites mainly as a very low permeable formation and are then considered as the regional aquitard.

5.4 Difference between hydrological watershed and hydrogeological watershed

The continuity of andesitic lava flows $^2\alpha$ along the resistivity cross-sections (Fig. 7), from north to south and especially under the “Morne Jeanette” (C5), clearly suggests a continuity of groundwater flow beyond the Duclos River watershed and in direction of the Fond Lahaye watershed. This hypothesis of a clear difference between hydrological watershed and hydrogeological watershed is supported by (1) the piezometric fluctuations (Fig. 4), showing that Fond Lahaye upper borehole is in a captive aquifer with multiannual dynamic fluctuations, (2) groundwater mineralization and long duration time transfers (> 50 years by CFC groundwater datation, Gourcy et al., 2009) and (3) the high flowrates of Fond Lahaye Boreholes (more than $1.2 \cdot 10^6 \text{ m}^3/\text{year}$ have been calculated by Ollagnier et al., 2007; Vittecoq et al., 2008; Vittecoq et Arnaud, 2014).

5.6 Geothermal insights

The very low resistivity (6-10 ohm m) of Hyaloclastites 1H , cannot correspond to actual salt water intrusion as they are situated higher above sea level, but could be linked to the period during which they remains submarine before volcanic uplift during the Carbet Pitons volcanic phase (0.8 – 1.2 Ma). On another side, or in addition, their very low resistivity could be an evidence that these hyaloclastites are a hydro-thermalized caprock of an underneath geothermal system. The two thermal springs (Didier – 32°C , $1850 \mu\text{S cm}^{-1}$ and Absalon – 36°C , $1730 \mu\text{S cm}^{-1}$) could be leaks of this geothermal system, through hydro-thermalized faults allowing the rise of mineralized gaseous waters (it must be noticed that the supposed fault interpreted in Fig. 6 (C2 – 2800 m) is aligned with Didier springs, Absalon springs and with the Alma and Dumauzé Dacitic Domes).



Then, geothermal fluid circulations could follow four steps: (1) deep infiltration of effective rainfall through andesitic domes ($^{\circ}\alpha$ bi) and associated deep rooting and deep mixing, (2) interaction with CO_2 and ascent along faults, (3) mixing with andesitic aquifer $^2\alpha$, and (4) emergence in thermal springs. The flowrate of these springs being relatively low, we can state that a part of the ascending enriched fluids do not emerge at the surface, and flow and diffuse in the andesitic aquifer $^2\alpha$. The higher groundwater mineralization downstream ($1000 \mu\text{S cm}^{-1}$ in Fond Lahaye boreholes), compared to the range of water electrical conductivity of cold springs and rivers ($50\text{-}200 \mu\text{S cm}^{-1}$) emerging from the aquifers upstream (cf. Table 1), clearly support this hypothesis.

6 – Discussion

Heliborne Time Domain ElectroMagnetic data reveals in depth resistivity contrasts whose interpretation with boreholes and springs data allowed constraining a detailed hydrogeological conceptual model. Working at the watershed scale brings new elements of hydrogeological functioning of andesitic volcanic complex. Vessel and Davis (1981), Bogie and Mackenzie (1998) and Selles et al., (2015) proposed a geological conceptual model of andesitic stratovolcanoes putting in evidence central (0-2 km from the vent), proximal (5-10 km), medial (10-15 km) and distal (15-40 km) facies variations. The originality of our work is to focus on improving hydrogeological functioning of central and proximal parts of such andesitic system. Indeed, medial and distal parts, on which hydrogeological researches are generally focused on continental volcano (Selles, 2014), corresponding to lower and accessible area, are in our case further under the sea.

On the scale of the island of Martinique, the proposed hydrogeological functioning, conceptual model (and also our methodology) could likely been extended to the other watersheds situated on the Carbet volcanic complex and on the Morne Jacob shield volcano. Extrapolation to the entire Martinique is nevertheless not considered, as a specific hydrogeological functioning has been demonstrated for the centre of the Island (Vittecoq et al., 2015), as effective rainfall is significantly lower ($<1500 \text{ mm}$) in the southern half of the island (Vittecoq et al., 2010) and because our conceptual model, concerning mainly fissured and fractured lava, could not fit with the Mount Pelée stratovolcano located in the North of Martinique (covering 15% of the Martinique area) and constituted by pyroclastic flows (Traineau et al., 1989).

Secondly, our conceptual model could also enhance, with new insights, existing characterization of the hydrogeology of small volcanic Islands and especially West Indies and Caribbean volcanic Islands (Unesco, 1986; Falkland and Custodio, 1991; Davies and Peart, 2003, and Robins, 2013). However, Hemmings et al., (2015), studying Montserrat Island, an andesitic island located in the Lesser Antilles, concluded that they didn't know which model between Hawaiian and Canarian model could fit with Montserrat island. As both were concerning only basaltic islands, other models have to be proposed. Our conceptual model, thanks to the high-resolution heliborne geophysical survey and correlations with geological and hydrogeological data, could then help better understanding hydrogeological functioning of other Lesser Antilles andesitic islands. For instance, the threefold division of West Indies hydrogeological classification by Robins et al., (1990) could be updated with a fourth category considering groundwater in permeable perched high-rise volcanic dome and in underneath fractured volcanic rocks.



The main geological structures highlighted lead to preferential flow circulations and to a non-adequacy between hydrogeological and topographical watersheds, as supposed by Charlier et al., (2011) at a smaller scale (45 ha) in Guadeloupe. The consequence is that even if the topographical watershed is small, underground flow circulations can add significant amount of water to river watershed's water balance, if aquifers are situated above (in elevation or upstream). We thus support the
5 necessity to include and characterize neighboring watersheds to extend our methodology and results to others areas or islands. This can be even emphasized if lava domes and associated roots are situated upstream, as they present very high hydraulic conductivity leading to vertical in depth preferential flow circulations.

Correlations between resistivity and geological data also show that, within the interval 10 ohm m to 500 ohm m for resistivity, and with a range of 0.9 Ma and 5.5 Ma for ages, the younger the formations, the higher their resistivity. This correlation was
10 also evidenced by Vittecoq et al., (2014) for a basaltic island (5 to 100 ohm m – 1 to 8 Ma). Correlations between resistivity, geology and transmissivity/hydraulic conductivity data of three aquifers suggest another relation: the older the formation, the higher its transmissivity (and the lower its resistivity). This correlation is reinforced by adding the results of Vittecoq et al., (2015) obtained on an older aquifer (15 Ma) on Martinique Island, with higher hydraulic conductivity and lower resistivity
15 than the ones observed in the present study. This correlation is also the opposite of the relationship for basaltic island (Custodio et al., 2004, Vittecoq et al., 2014) due, as exposed by Vittecoq et al., (2015), to the influence of tectonic fracturing in subduction zones associated to andesitic volcanic islands, which rejuvenate or increase aperture of the ancient fractures.

The accuracy of correlations between boreholes and TDEM soundings is highly dependent on the distance to the nearest TDEM flight line. Accordingly, a particular attention must be paid to the way this comparison is achieved, mainly in terms of distance and elevation difference. This being said, heliborne geophysical survey is certainly the best-cost efficiency method, and
20 probably the only method providing this density of data down to 200 m depth, allowing a detailed geological and hydrogeological characterization at this working scale. Nevertheless a minimum of ground based geological and hydrogeological data are necessary, thanks to bore-wells.

7 – Conclusion

From an operational point of view, our data and results should be very helpful for local stakeholders facing environmental
25 impacts and overexploitation of the Case Navire River. We show that large volumes of water infiltrate and flow in several aquifers. Sustainable management of water resources will require a better repartition between rivers and aquifers. Aquifers, and especially downstream the watersheds, could be exploited in order to decrease the use of the dams, especially in dry seasons. Future drillings programs could be launched, considering our conceptual model. We also provide some insights about potential geothermal resources such as the pathway of deep infiltrated water through the roots of the andesitic dome, the
30 presence of a low resistivity regional aquitard and the link with the thermal springs.



In conclusion, our multidisciplinary approach and results allow characterizing in detail the hydrogeological functioning and characteristics of the main aquifer and aquitard units, leading to the proposition of a hydrogeological conceptual model of an andesitic island at the watershed scale, putting in evidence the key role of geological structures and volcanic domes on groundwater flows. We also demonstrate, for the studied geological formations, that hydraulic conductivity increase with age in this andesitic-type volcanic island. Moreover, the working scale seems particularly suitable for due to the complexity of edifices, with heterogeneous geological formations presenting high lateral and vertical variability. Andesitic-type volcanic island being little known and studied, our work offers, in addition to the proposed conceptual model and thanks to the high-resolution heliborne geophysical survey, new guidelines for accurate correlations between resistivity, geology and hydraulic conductivity for other volcanic islands.

10 8 – Acknowledgments

This paper is a contribution of “DemosTHEM” and “Karibo” BRGM Research programs. Previous investigations made by BRGM over the studied watersheds were co-funded by CACEM, ODE and BRGM. The heliborne geophysical survey, called “MartEM” program (Deparis et al., 2014), was co-funded by BRGM, the FEDER funds for Martinique, the Regional Office for Environment Planning and Housing (DEAL), the Regional Council, and the Water Office of Martinique (ODE).

15 References

- Auken E., Christiansen A.V., Westergaard J.H. Kirkegaard C., Foged N., and Viezzoli A.: An integrated processing scheme for high-resolution airborne electromagnetic surveys, the SkyTEM system. *Exploration Geophysics*, 40,184-192, 2009.
- Bogie, I., and Mackenzie, K.: The application of a volcanic facies model to an andesitic stratovolcano hosted geothermal system at Wayang Windu, Java, Indonesia. In: *Proceedings 20th NZ Geothermal Workshop*, pp. 265–270, 1998.
- 20 Boudon, G., Le Friant, A., Komorowski, J.C., Deplus, C., and Semet, M.P.: Volcano flank instability in the Lesser Antilles arc: diversity of scale, processes, and temporal recurrence. *Journal of Geophysical Research- Solid Earth* 112 (B8), 2007.
- Charlier, J.B., Lachassagne, P., Ladouche, B., Cattani, Ph, Moussa, R. and Voltz, M.: Structure and hydrogeological functioning of an insular tropical humid andesitic volcanic watershed: a multi-disciplinary experimental approach. *J. Hydrol.*, 398, 155–170. doi:10.1016/j.jhydrol.2010.10.006, 2011.
- 25 Christiansen, A.V. and Auken, E.: A global measure for depth of investigation. *Geophysics*, 77, WB171-WB177, 2012.
- Cruz, J.V.: Groundwater and volcanoes: examples from the Azores archipelago. *Environ. Geol.* 44, 343–355, 2003.
- Cruz, J.V. and Silva, M.O.: Hydrogeologic framework of Pico Island, Azores, Portugal. *Hydrogeol. J.* 9 (2), 177–189, 2001.
- Custodio, E.: Hydrogeologia de las rocas volcánicas. 3rd UNESCO-ESA-IHA Symposium on Groundwater, pp. 23–69, 1975.
- Custodio, E.: Hydrogeology of volcanic rocks. In: UNESCO (Ed.), *Groundwater Studies. An International Guide for*
- 30 *Hydrogeological Investigations*, Paris, 423pp, 2005.



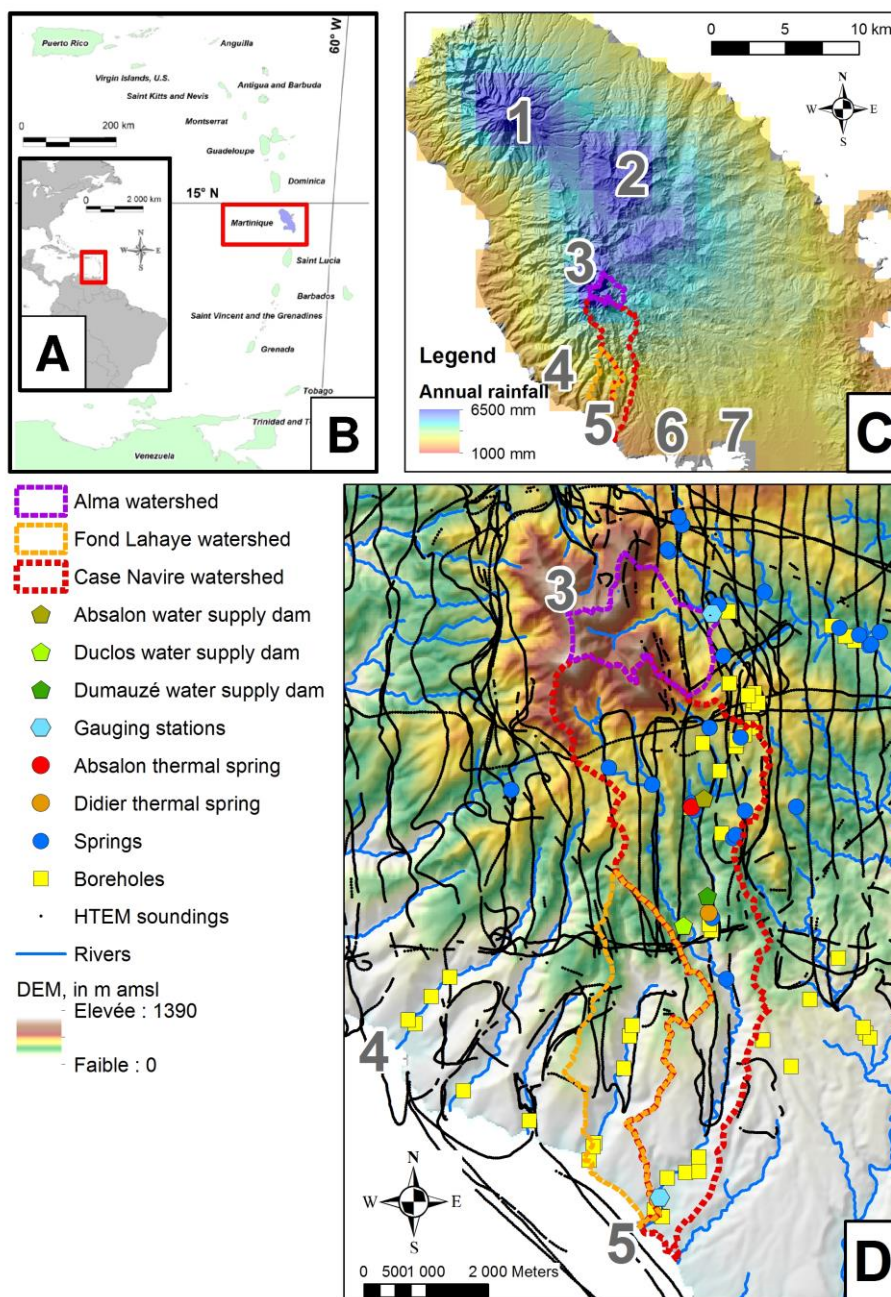
- Custodio, E., Lopez Garcia, L. and Amigo, E.: Simulation par modèle mathématique de l'île volcanique de Ténériffe (Canaries, Espagne). *Hydrogéologie* 1988 (2), 153–167, 1988.
- Davies, J. and Peart, R.J.: A Review of the Groundwater Resources of Central and Northern Montserrat. British Geological Survey Commissioned Report, CR/03/257C. 87pp, 2003.
- 5 Deparis, J., Reninger, P.A., Perrin J., Martelet G. and Audru, J.C.: Acquisition géophysique hélicoptée de la Martinique. Openfile BRGM Report RP-62428-FR. <http://infoterre.brgm.fr/rapports/RP-62428-FR.pdf>, 2014.
- Falkland, A. and Custodio, E.: Guide on the hydrology of small islands. Studies and reports in hydrology 49. UNESCO, Paris, pp 1–435, 1991.
- Gadalia A., Rad, S. and Tailame, A.L.: Compléments d'exploration géothermique : volet géochimie des fluides. Openfile
10 BRGM Report RP-62710-FR, 2014.
- Germa, A., Quidelleur, X., Labanieh, S., Lahitte, P. and Chauvel, C.: The eruptive history of Morne Jacob volcano (Martinique Island, French West Indies): geochronology, geomorphology and geochemistry of the earliest volcanism in the recent Lesser Antilles arc. *J. Volcanol. Geotherm. Res.* 198, 297–310, 2010.
- Germa, A., Quidelleur, X., Labanieh, S., Chauvel, C. and Lahitte P.: The volcanic evolution of Martinique Island: Insights
15 from K–Ar dating into the Lesser Antilles arc migration since the Oligocene. *Journal of Volcanology and Geothermal Research*, 208 (2011), pp. 122–135, 2011.
- Gourcy, L., Baran, N. and Vittecoq, B.: Improving the knowledge of pesticide and nitrate transfer processes using age dating tools (CFC, SF₆, 3H) in a volcanic island. *Journal of Contaminant Hydrology*, 108(3-4), 107-117. doi:10.1016/j.jconhyd.2009.06.004, 2009.
- 20 Guiscafre, J., Klein J.C. and Moniod, F.: Les ressources en eau de surface de la Martinique. Monographies hydrologiques ORSTOM, 1976.
- Hagedorn, B., El-Kadi, A.I., Mair, A., Whittier, R.B. and Ha, K.: Estimating recharge in fractured aquifers of a temperate humid to semiarid volcanic island (Jeju, Korea) from water table fluctuations, and Cl, CFC-12 and 3H chemistry. *J. Hydrol.* 409 (3–4), 650–662, 2011.
- 25 Hamm, S.-Y., Cheong, J.-Y., Jang, S., Jung, C.-Y. and Kim, B.-S.: Relationship between transmissivity and specific capacity in the volcanic aquifers of Jeju Island, Korea. *J. Hydrol.* 310, 111–121, 2005.
- Join, J.-L., Folio, J.-L. and Robineau, B.: Aquifers and groundwater within active shield volcanoes. Evolution of conceptual models in the Piton de la Fournaise volcano. *J. Volcanol. Geoth. Res.* 147 (1–2), 187–201, 2005.
- Macdonald, G.A., Abbott, A.T. and Peterson, F.L.: Volcanoes in the sea. The geology of Hawaii. University of Hawaii Press,
30 Honolulu, 571pp, 1983.
- Ollagnier, S., Brugeron, A., Vittecoq, B. and Petit, V.: Caractérisation du fonctionnement hydrodynamique et analyse qualitative de la nappe d'eau souterraine de Schœlcher-Case Navire. Openfile BRGM Report BRGM/RP-55458-FR, 2007.
- d'Ozouville, N., Auken, E., Sorensen, K.I., Violette, S. and de Marsily, G.: Extensive perched aquifer and structural implications revealed by 3D resistivity mapping in a Galapagos volcano. *Earth and Planetary Sc. Letters*, 269, 517-521, 2008.



- Peterson, F.L.: Water development on tropic volcanic islands. Type example: Hawaii. *Ground Water* 10(5), 18–23, 1972.
- Pryet, A., D’ozouville, N., Violette, S., Deffontaines, B., and Auken, E.: Hydrogeological settings of a volcanic island (San Cristobal, Galapagos) from joint interpretation of airborne electromagnetics and geomorphological observations. *Hydrology and Earth System Sciences*, Volume 16, no. 12, 4571–4579, 2012.
- 5 Reninger, P.-A., Martelet, G., Deparis, J., Perrin, J. and Chen, Y.: Singular value decomposition as a denoising tool for airborne time domain electromagnetic data. *J. Appl. Geophys.* 75, 264–276. <http://dx.doi.org/10.1016/j.jappgeo.2011.06.034>, 2011.
- Reninger, P.A., Martelet, G. and Perrin, J.: Frame effective tilt correction for HEM data acquired over rugged terrain. First European Airborne Electromagnetics Conference Near Surface Geoscience 2015, Sep 2015, Turin, Italy. DOI: 10.3997/2214-4609.201413865, 2015.
- 10 Reninger, P.A., Martelet, G., Perrin, J. and Dumont, M.: Reprocessing of regional AEM surveys for geological, hydrogeological and geotechnical applications. AEM2018 - 7th international Workshop on Airborne Electromagnetics. Kolding, Denmark, 2018.
- Selles, A.: Multidisciplinary study about the hydrogeological behavior of the Eastern flank of Merapi volcano, Central Java, Indonesia. PhD Thesis Université Paris 6 Pierre et Marie Curie, France, 2014.
- 15 Selles, A., Deffontaines, B., Hendrayana, H. and Violette, S.: The eastern flank of the Merapi volcano (Central Java, Indonesia): Architecture and implications of volcanoclastic deposits. *Journal of Asian Earth Sciences* 108 (2015) 33–47, 2015.
- Senergues, M.: Suivi géologique et hydrogéologique de deux forages de reconnaissance sur le site de Fond Baron, commune de Fort-de-France. Openfile BRGM Report BRGM/RP-62782-FR, 2014.
- Sigurðsson, F. and Einarsson, K.: Groundwater resources of Iceland. Availability and demand. *Jökull* 38, 35-54, 1988.
- 20 Sørensen, K.I. and Auken, E.: SkyTEM - A new high-resolution helicopter transient electromagnetic system. *Explor. Geophys.*, 35, 191–199, 2004.
- Traineau, H., Westercamp, D. and Benderitter, Y.: Case study of a volcanic geothermal system. Mount Pelée, Martinique. *J. Volcanol. Geotherm. Res.*, vol. 38, p. 49-66, 1989.
- Unesco: First workshop on the hydrogeological atlas of the Caribbean Islands. Santo Domingo 7-10 october 1986. Final
- 25 Report, 1986.
- Vessel, R.D. and Davis, D.K.: Nonmarine sedimentation in an active fore arc basin. In: Ethridge, F.G., Flores, R.M. (Eds.), *Recent and Ancient Nonmarine Depositional Environments: Models for Exploration: Society of Economic Paleontologists and Mineralogists Special Paper 31*, pp. 31–45, 1981.
- Viezzoli, A., Christiansen, A.V., Auken, E. and Sørensen, K.: Quasi-3D modeling of airborne TEM data by spatially
- 30 constrained inversion. *Geophysics*, 73, F105-F113, 2008.
- Violette, S., Ledoux, E., Goblet, P. and Carbonnel, J.P.: Hydrologic and thermal modeling of an active volcano: the Piton de la Fournaise, Réunion. *J. Hydrol.* 191, 37–63, 1997.
- Violette, S., d’Ozouville, N., Pryet A., Deffontaines, B., Fortin, J. and Adelinet, M.: Hydrogeology of the Galapagos Archipelago: an integrated and comparative approach between islands. In K. S. Harpp, E. L. Mittelstaedt, N. D’Ozouville, and



- D. W. Graham (Eds.), *The Galápagos as a Laboratory for the Earth Sciences*, Chapter 9, 167-183. American Geophysical Union, Washington, D.C. ISBN: 978-1-118-85241, 2014.
- Vittecoq B. and Arnaud L.: Évaluation du débit d'exploitation durable du forage 177ZZ0181/CNF3 de Case Navire, commune de Schoelcher (Martinique). Openfile BRGM Report BRGM/RP-63077-FR, 2014.
- 5 Vittecoq, B., Lachassagne, P., Lanini, S., Ladouche, B., Marechal, J.C. and Petit, V.: Elaboration d'un système d'information sur les eaux souterraines de la Martinique: identification et caractérisations quantitatives. Openfile BRGM Report RP-55099-FR. <http://infoterre.brgm.fr/rapports/RP-55099-FR.pdf>, 2007.
- Vittecoq, B., Lachassagne, P., Lanini, S. and Maréchal, J.C.: Evaluation des ressources en eau de la Martinique : calcul spatialisé de la pluie efficace et validation à l'échelle du bassin-versant. *Revue des Sciences de l'Eau* 23 (4), 361–373, 2010.
- 10 Vittecoq, B., Deparis, J., Violette, S., Jaouen, T. and Lacquement, F.: Influence of successive phases of volcanic construction and erosion on Mayotte Island's hydrogeological functioning as determined from a helicopter-borne resistivity survey correlated with borehole geological and permeability data. *J. Hydrol.*, 509, 519–538. <http://dx.doi.org/10.1016/j.jhydrol.2013.11.062>, 2014.
- Vittecoq, B., Reninger, P.A., Violette, S., Martelet, G., Dewandel, B. and Audru, J.C.: Heterogeneity of hydrodynamic properties and groundwater circulation of a coastal andesitic volcanic aquifer controlled by tectonic induced faults and rock fracturing – Martinique Island (Lesser Antilles - FWI). *J. Hydrol.*, 529, 1041-1059. <http://dx.doi.org/10.1016/j.jhydrol.2015.09.022>, 2015.
- 15 Westercamp, D., Andreieff, P., Bouysse, P., Cottez, S. and Battistini, R., Notice explicative, Carte géol. France (1/50 000), feuille Martinique – Orléans : Bureau de recherches géologiques et minières, 246 p, 1989.
- 20 Westercamp, D., Pelletier, B., Thibaut, P.M., Traineau, H. and Andreieff, P.: Carte géologique de la France (1/50.000), feuille Martinique. BRGM. <http://infoterre.brgm.fr/>, 1990.
- Won, J.-H., Kim, J.-W., Koh, G.-W. and Lee, J.-Y.: Evaluation of hydrogeological characteristics in Jeju Island, Korea. *Geosci. J.* 9 (1), 33–46, 2005.
- 25 Won, J.-H., Lee, J.-Y., Kim, J.-W. and Koh, G.-W.: Groundwater occurrence on Jeju Island, Korea. *Hydrogeol. J.* 14, 532–547, 2006.



5 **Figure 1: The Location of the island of Martinique (A) on the scale of the America and (B) on the scale of the Lesser Antilles. Location of the watersheds (C) on the scale of the northern part of Martinique Island. (1) Mount Pelée, (2) Morne Jacob shield volcano, (3) Carbet volcanic complex, (4) Case Pilote city, (5) Schoelcher city, (6) Fort-de-France city, (7) Lamentin city. (D) Location of rivers, water supply dams, gauging stations, watershed, thermal springs, cold springs, boreholes and HTEM soundings along flight lines.**

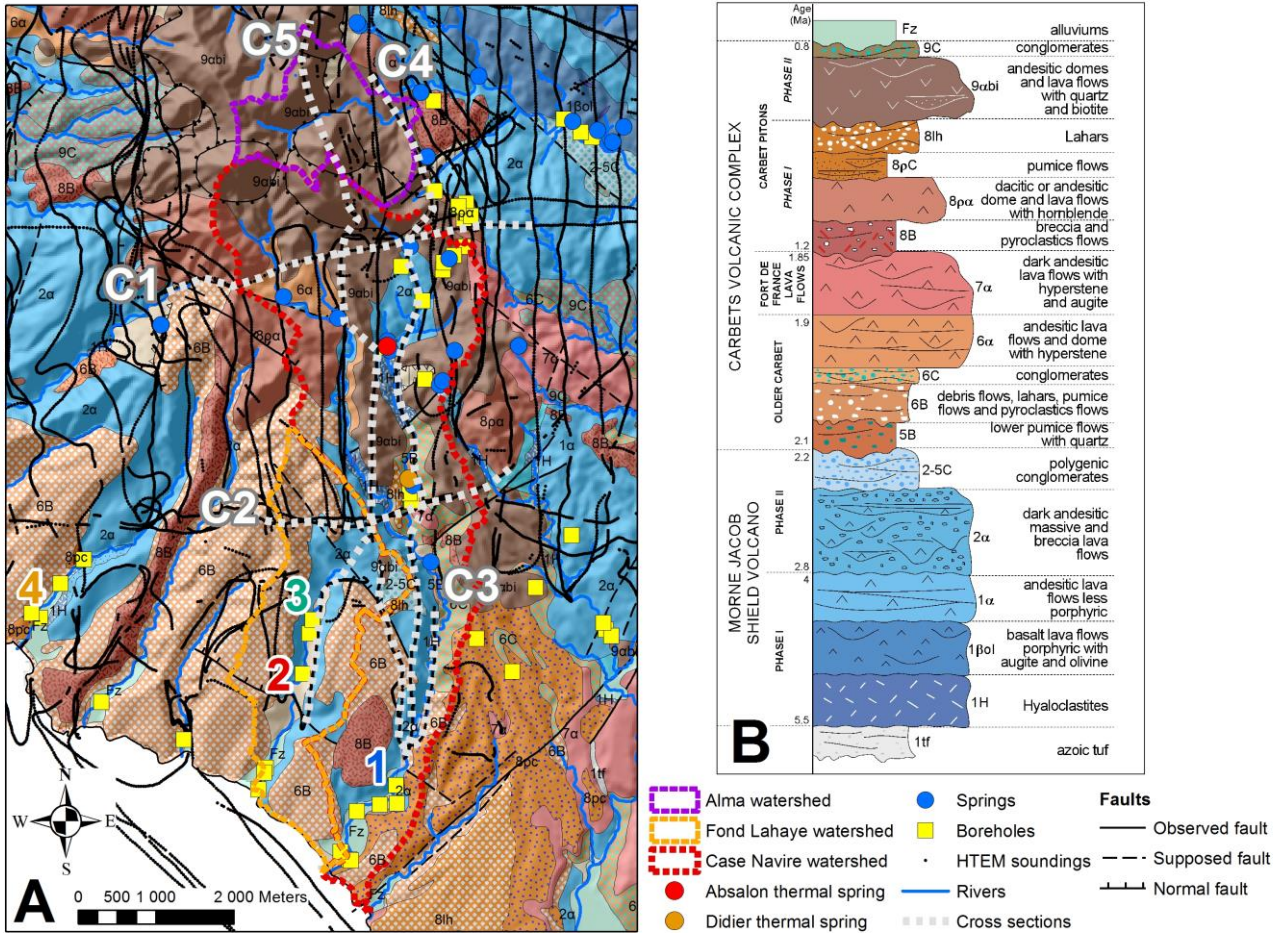


Figure 2: (A) Geological map (adapted from Westercamp et al., 1990) of the studied watersheds and (B) strato-lithological scale. Location of the piezometers (piezometric chronicles on Fig. 4): (1) Case Navire, National number 1177ZZ0165, (2) Fond Lahaye National number 1177ZZ0161, (3) Fond Lahaye National number 1177ZZ0177 and (4) Case Pilote National number 1177ZZ0173. Cross-section location in white (Cross-sections on Fig. 6 and 7).

5

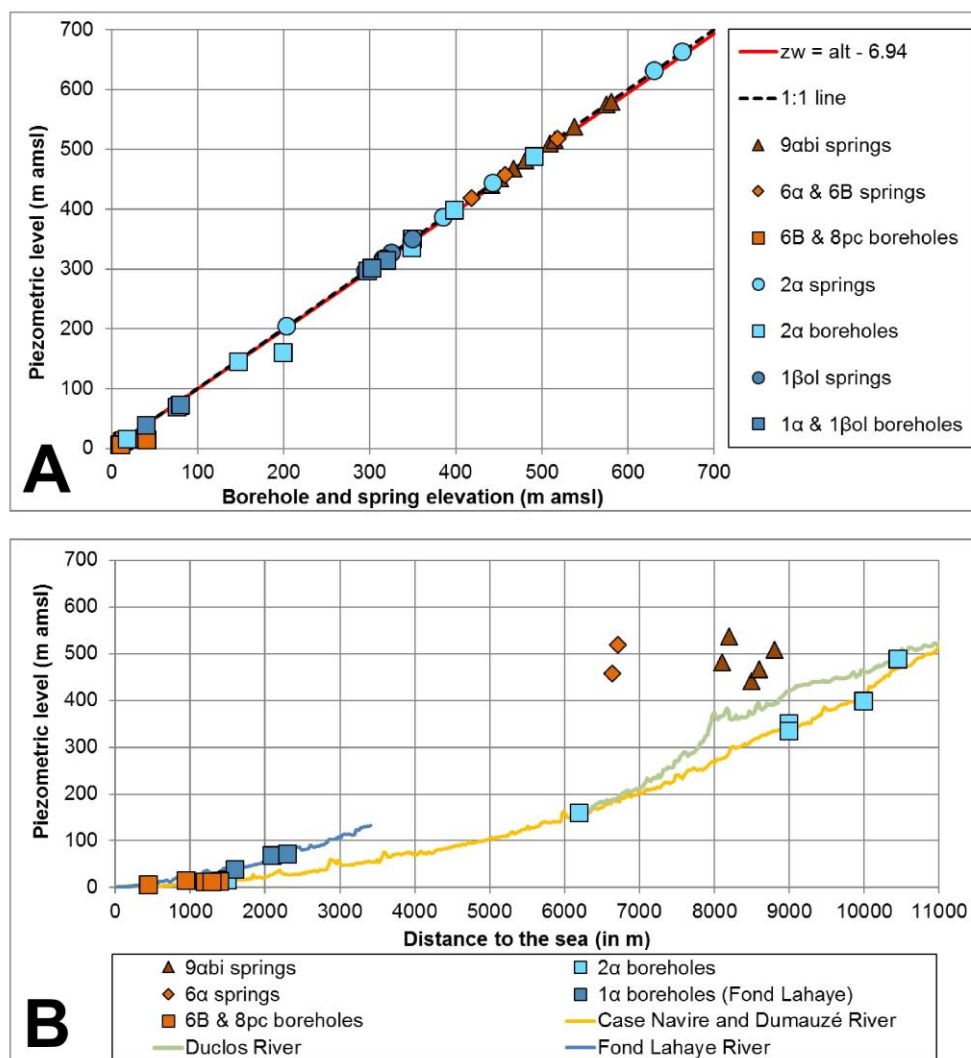


Figure 3: (A) Comparison between borehole and spring elevation and associated piezometric level (for twenty-six boreholes). The piezometric level is on average seven meters below ground level, following this linear relationship: $zw = elev - 6.94$ ($R^2=0.99$), where 'zw' is the piezometric level (m) and 'elev' the elevation (m). (B) Topographic profiles of Case Navire, Dumauzé, Duclos and Fond Lahaye rivers, the piezometric levels of boreholes in the associated watersheds with the lithology of the aquifer, and the elevation and lithology of the aquifer of springs.

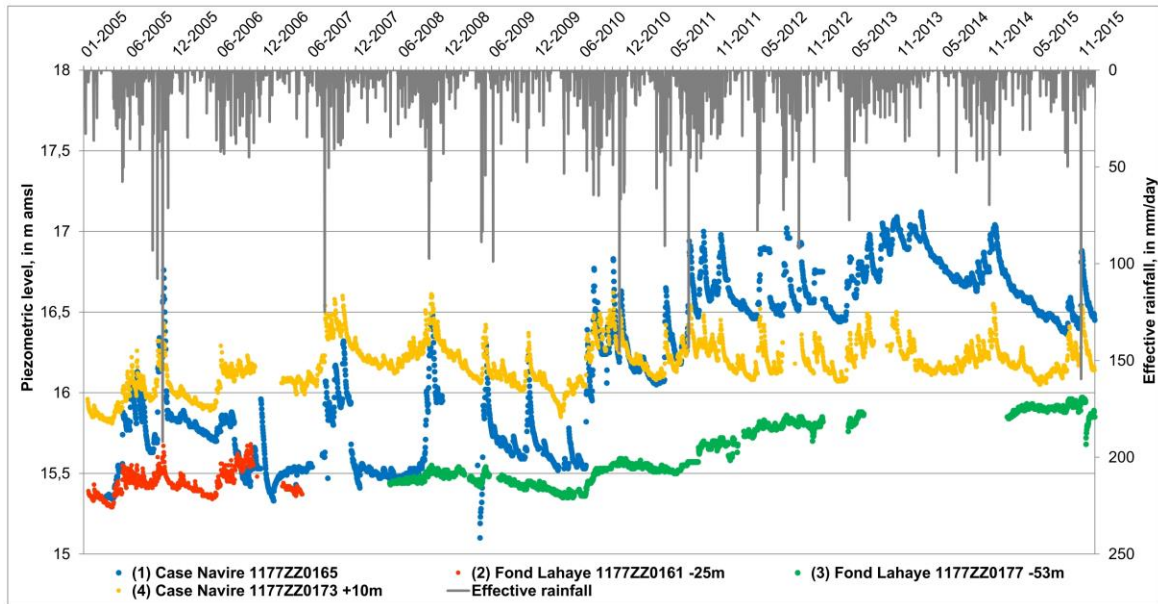
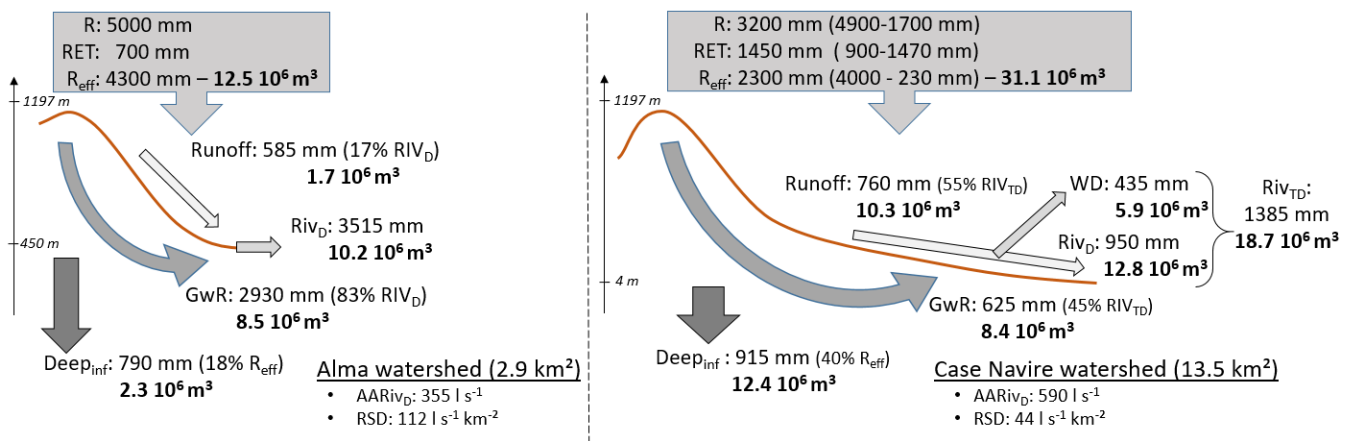


Figure 4: Piezometric levels (monitored in the framework of the European piezometric network) and effective rainfall monitoring between 2005 and 2015. The first piezometer is located on the Case Navire watershed (1 on Fig. 2A), the two next are on the Fond Lahaye watershed (2 and 3 on Fig. 2A) and the last one is in Case Pilote city (4 on Fig. 2A), three kilometers west of Fond Lahaye.

5 Piezometric levels of piezometers 2, 3 and 4 have been modified to fit on the same graph (by -25m, -53m and +10m compare to their initial value, respectively).



10 Figure 5: Annual water balance of the three watersheds: Case-Navire, Alma and Fond Lahaye. Rainfall (R), Real Evapo-Transpiration (RET) and Effective Rainfall (Reff) are from Vittecoq et al., (2010) and Arnaud et al., (2013). Average annual river discharge (AARivD) and river specific discharge (RSD) are calculated from gauging stations. Runoff: Reff contribution to river discharge. WD: volume of water for the drinking water distribution system. RivD: river discharge. RivTD: river total discharge (=RivD+WD). GwR: Groundwater contribution to river discharge. Deepinf: deep groundwater flow.

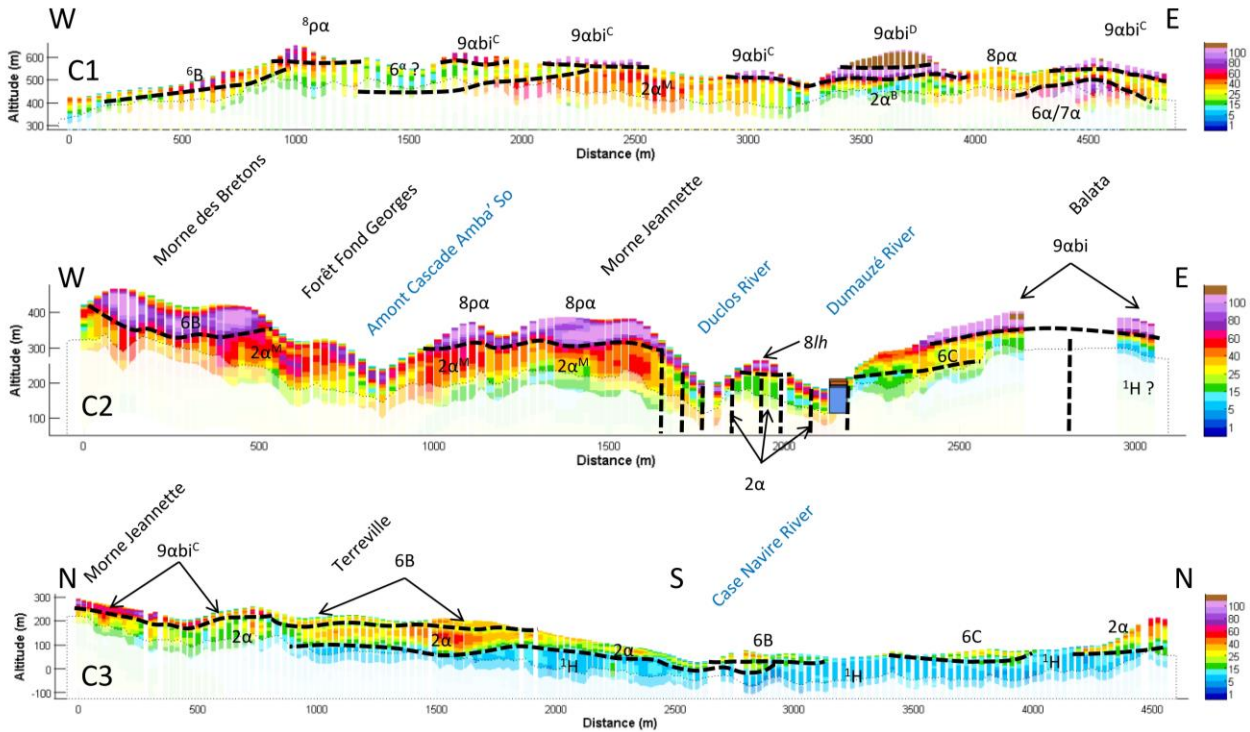


Figure 6: Internal resistivity and hydrogeological structure along 3 cross-sections: C1, C2 and C3

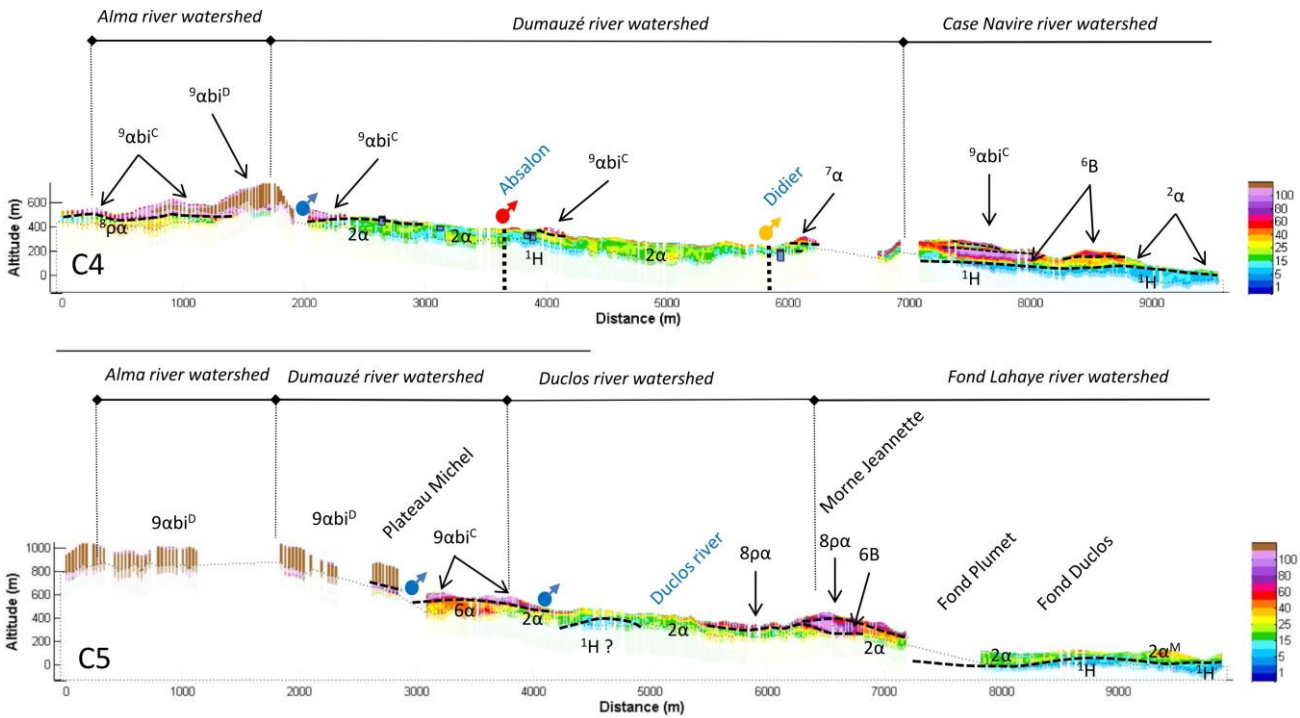


Figure 7: Internal resistivity and hydrogeological structure along 2 cross-sections: C4 and C5

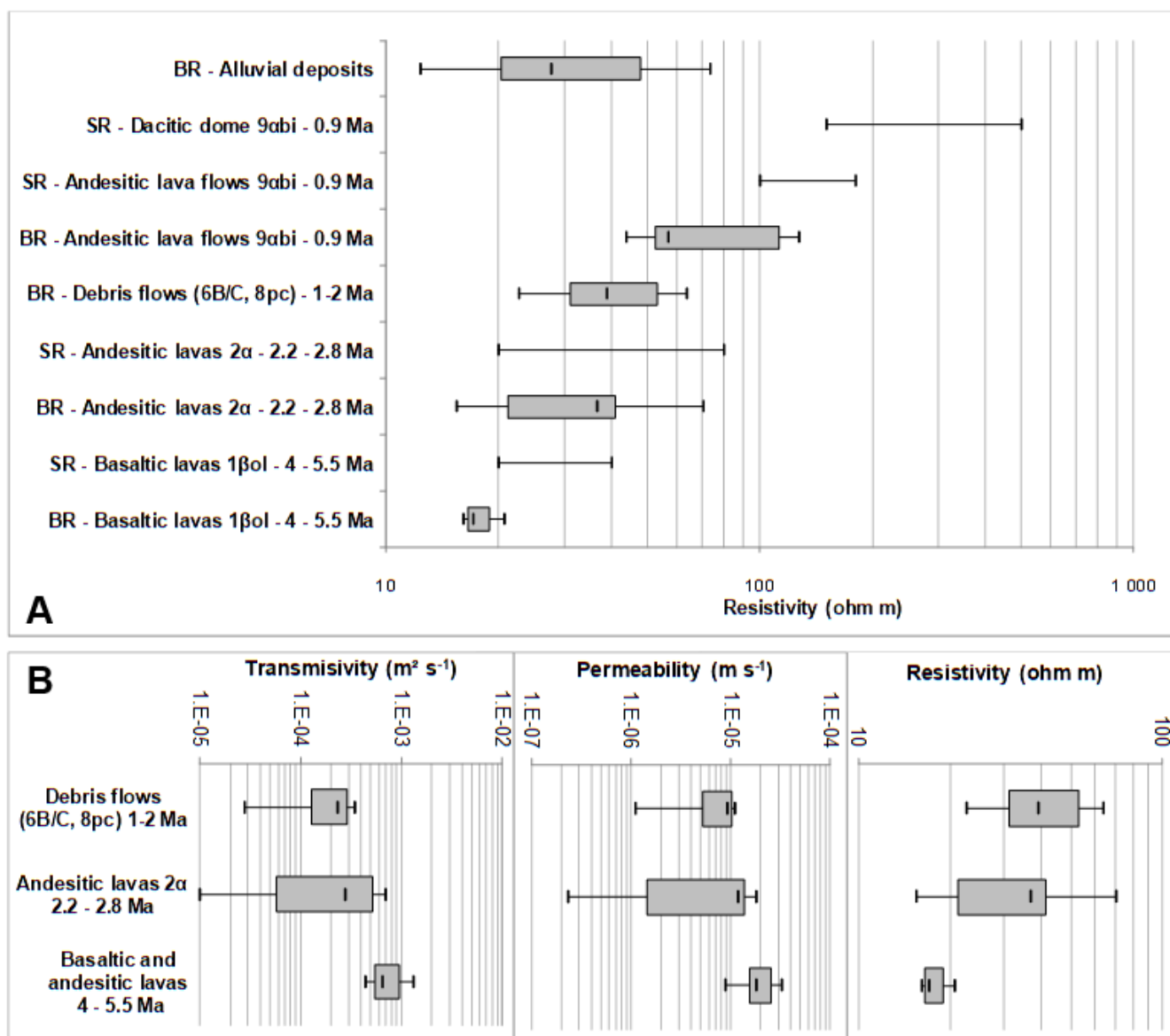


Figure 8: (A) Boreholes (BR) and springs (SR) resistivity ranges according to their lithological facies and age (Fig. 2). The younger the formation, the higher its resistivity. (B) Comparison between transmissivity, permeability and resistivity for three aquifer formations considering boreholes values.

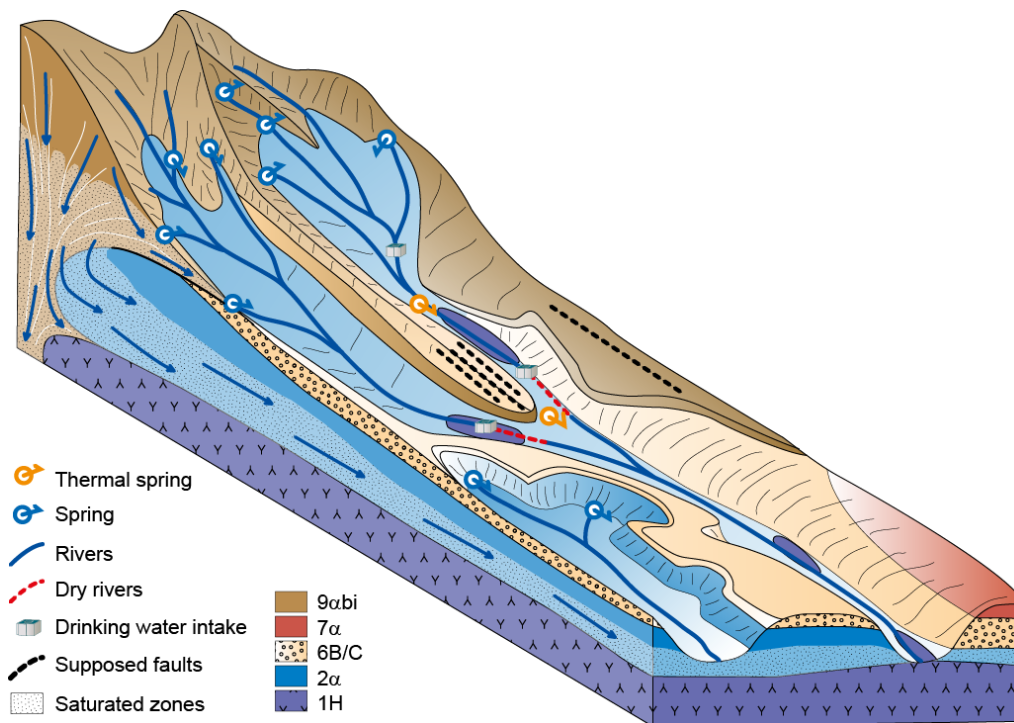


Figure 9: Hydrogeological conceptual model.

Code	Lithological	Age (Ma)	Thickness (m)	Resistivity ranges ohm.m (Q1-Q3)	Aquifer typology	Porosity	Transmissivity ($m^2 s^{-1}$)			Hydraulic conductivity ($m s^{-1}$)		Water electrical conductivity $\mu S cm^{-1}$		
							Nbr. of boreholes	range	Average and std.	range	Average and std.	Nbr. Of springs	Springs	Rivers
$9\alpha bi$	$9\alpha bi^D$ - Andesitic domes	0.9	> 500	Springs : 150 - 500	Upper major perched aquifer	highly fissured/fractured	-	-	-	-	-	6	106 - 156	111
	$9\alpha bi^C$ - andesitic lava flows	0.9	10 - 100	Springs: 100 - 180 Boreholes: 50 - 100	Upper minor perched aquifer	highly fissured/fractured	-	-	-	-	-	-	-	124 - 142
$8\alpha a$	Andesitic and dacitic domes and lava flows	1	10 - 100	70 - 120	Minor perched aquifer	Fissured/fractured	-	-	-	-	-	-	-	-
$6B/C$	Breccias, debris flow from the first phase of construction of the old Carbet	2	100 - 200	20 - 40	Minor perched aquifer	Heterogeneous Locally aquitard (cemented breccias)	3	$2.3 \cdot 10^{-4}$ to $3.7 \cdot 10^{-4}$	$2.9 \cdot 10^{-4}$ std: $5.8 \cdot 10^{-5}$	$6.7 \cdot 10^{-6}$ to $1.7 \cdot 10^{-5}$	$1.1 \cdot 10^{-5}$ std: $4.6 \cdot 10^{-6}$	-	-	-
2α	Andesitic lava flows	2.2 - 2.8	100 - 300	- $2\alpha^M$ (massive parts): 30 - 70 - $2\alpha^f$ (fissured and fractured parts): 15 - 30 - $2\alpha^B$ (breccias and autoclásticos parts): 10 - 15	Major aquifer	Heterogeneous	9	$1.0 \cdot 10^{-5}$ to $7.0 \cdot 10^{-4}$	$3.3 \cdot 10^{-4}$ std: $2.4 \cdot 10^{-4}$	$2.3 \cdot 10^{-7}$ to $1.8 \cdot 10^{-5}$	$9.0 \cdot 10^{-6}$ std: $6.4 \cdot 10^{-6}$	7	50 - 200	91 - 120
$1\beta ol$	basaltic lavas	4 - 5.5	100 - 300	16 - 20	Major aquifer	Fissured/fractured	7	$4.4 \cdot 10^{-4}$ to $1.3 \cdot 10^{-3}$	$7.7 \cdot 10^{-4}$ std: $2.9 \cdot 10^{-4}$	$8.8 \cdot 10^{-6}$ to $3.3 \cdot 10^{-5}$	$2.0 \cdot 10^{-5}$ std: $7.5 \cdot 10^{-6}$	-	-	91 - 98
$1H$	hyaloclastites	4 - 5.5	> 200	6 - 10	Regional aquitard	very low permeable formation	-	-	-	-	-	-	-	-

5

Table 1: Geological, geophysical and hydrogeological characteristics of the main aquifer and aquitard formations.